Acta Crystallographica Section F
Structural Biology and Crystallization Communications
ISSN 1744-3091

Crystallization and preliminary X-ray diffraction studies of Seneca Valley Virus-001, a new member of the *Picornaviridae* family

Sangita Venkataraman,[a] Seshidhar P. Reddy,[b] Jackie Loo,[a] Neeraja Idamakanti,[b] Paul L. Hallenbeck[b] and Vijay S. Reddy[a]*

[a]Department of Molecular Biology, The Scripps Research Institute, La Jolla, CA 92037, USA, and [b]Neotropix Inc., 351 Phoenixville Pike, Malvern, PA 19355, USA

Correspondence e-mail: reddyv@scripps.edu

Received 23 December 2007
Accepted 12 March 2008

Seneca Valley Virus-001 (SVV-001) is a newly found species in the *Picornaviridae* family. SVV-001 is the first naturally occurring nonpathogenic picornavirus observed to mediate selective cytotoxicity towards tumor cells with neuroendocrine cancer features. The nonsegmented (+)ssRNA genome of SVV-001 shares closest sequence similarity to the genomes of the members of the *Cardiovirus* genus. However, based on the distinct characteristics of the genome organization and other biochemical properties, it has been suggested that SVV-001 represents a new genus, namely '*Senecavirus*', in the *Picornaviridae* family. In order to understand the oncolytic properties of SVV-001, the native virus was crystallized using the hanging-drop vapour-diffusion method. The crystals belonged to space group $R3$, with unit-cell parameters (in the hexagonal setting) $a = b = 311.5$, $c = 1526.4$ Å. Although the SVV crystals diffracted to better than 2.3 Å resolution, the data quality is acceptable [$I/\sigma(I) > 2.0$] to 2.6 Å resolution. The unit-cell volume and the locked rotation-function analysis suggest that six particles could be accommodated in the unit cell, with two distinct sets of one third of a particle, each containing 20 protomers, occupying the crystallographic asymmetric unit.

1. Introduction

The *Picornaviridae* family consists of non-enveloped positive-sense ssRNA viruses that infect a number of vertebrate hosts including humans. The family presently consists of nine genera that differ in structural and physicochemical properties (Stanway *et al.*, 2005). The viral genome contains ~7000 bp and is characterized by an internal ribosomal entry site (IRES) at the 5′ end and a poly(A) tail at the 3′ end (Semler & Wimmer, 2002). The picornavirus capsids are ~30 nm in diameter and are composed of 60 protomers arranged in a pseudo $T = 3$ icosahedral organization. Each protomer comprises VP1, VP2 and VP3 of MW 24–41 kDa and an internal protein, VP4, of MW 5.5–13 kDa (Semler & Wimmer, 2002). The capsids of most picornaviruses have depressions or canyons that are believed to aid in receptor binding and in escaping host immune surveillance (Rossmann, 1989). Picornaviruses are also known to recognize different types of receptors (Rossmann *et al.*, 2002). With the exception of cardioviruses, the family members possess short lipid moieties, also known as pocket factors, which are implicated in the uncoating of the virus during infection (Hadfield *et al.*, 1997).

SVV-001 is one of the new members of the *Picornaviridae*; its coat protein shares closest amino-acid sequence identity (35.8%) to the cardioviruses. SVV-001 was originally isolated as a contaminant during the cultivation of PER.C6 cells, which are transformed fetal retinoblast cells (Fallaux *et al.*, 1998; Reddy *et al.*, 2007), in the laboratory and is presumed to have been introduced *via* a bovine serum or porcine trypsin source. It was previously believed that SVV-001 could be a potential member of the *Cardiovirus* genus. However, based on the nature of the IRES and 2A protease, the lack of an internal poly(C) tract and the overall lack of sequence similarity to the members of the *Cardiovirus* genus, SVV-001 has been proposed to represent a new genus called '*Senecavirus*' (Knowles, 2007).

Table 1
Data-reduction statistics.

Values in parentheses are for the last resolution shell.

Space group	*R*3
Unit-cell parameters (hexagonal setting) (Å, °)	$a = b = 311.5$, $c = 1526.4$, $\alpha = \beta = 90$, $\gamma = 120$
Unit-cell parameters (rhombohedral setting) (Å, °)	$a = b = c = 533.0$, $\alpha = \beta = \gamma = 33.6$
Resolution range (Å)	92–2.3 (2.4–2.3)
Total No. of observations	19838366
No. of unique reflections	1968286
Wilson *B* factor (Å^2)	37.3
$I/\sigma(I)$	6.6 (0.9)
Completeness (%)	80.2 (37.1)
$R_{\rm merge}$ (%)†	23.3 (97.1)

† $R_{\rm merge} = \sum_{hkl}\sum_i |I_i(hkl) - \langle I(hkl)\rangle| / \sum_{hkl}\sum_i I_i(hkl)$, where $I_i(hkl)$ is the observed intensity and $\langle I(hkl)\rangle$ is the average intensity from multiple measurements of symmetry-related reflections.

The genomic RNA of SVV-001 (Genbank accession No. DQ641257) is infectious and comprises 7280 bases, excluding the poly(A) tail, encoding four structural proteins VP1–4 and seven nonstructural proteins that are derived from initial polyproteins. SVV-001 has a long 5′ untranslated region (UTR; 1–666) and a short 3′ UTR (7210–7280) (Hales *et al.*, 2006). The 5′ UTR is known to assume a cloverleaf-like secondary structure that matches the hepatitis C virus-like (IRES) element (Hellen & de Breyne, 2007).

Presently, the use of SVV-001 as an oncolytic agent is under Phase I/II trials (ClinicalTrials.gov identifier NCT00314925) and extensive research is ongoing to modify the virus/viral proteins for effective use and reuse (Reddy *et al.*, 2007). Hence, it is of importance and of interest to determine the three-dimensional structure of this novel picornavirus in order to gain better understanding of its role as an oncolytic agent. Additionally, it would be of interest to identify the structural features that distinguish it from other picornaviruses. The results of crystallization, data collection, processing and analysis of the diffraction data from the crystals of SVV-001 virions are reported in this paper.

2. Purification

Plaque-purified SVV-001 was grown in PER.C6 cells (Reddy *et al.*, 2007). The infected cells were lysed after ∼48 h to obtain a crude viral lysate that was subsequently centrifuged at 1500*g* for 10 min at 277 K. The resultant supernatant was then purified by ultracentrifugation using a caesium chloride (CsCl) step gradient (1.24 and 1.4 g ml^{-1}) followed by a continuous CsCl gradient (1.33 g ml^{-1}). At the end of each run, the light-scattering zone was collected from the gradient tubes. The purified virus was then dialyzed overnight against 1 l cold dialysis buffer [200 m*M* Tris–HCl, 50 m*M* HEPES pH 8.0, 10%(*v*/*v*) glycerol]. The virus concentration was determined by measuring the absorbance at 260 nm using a spectrophotometer, where one unit of optical density at 260 nm corresponds to 9.5×10^{12} particles (Reddy *et al.*, 2007). Fig. 1(*a*) shows the SDS–PAGE of the viral sample used for crystallization trials, highlighting the purity of the sample.

3. Crystallization

Crystallization trials were performed using the hanging-drop vapour-diffusion method at 293 K with the virus stock at a concentration of ∼10 mg ml^{-1}. The drop size was 4 µl, comprising 2 µl each of the virus and the reservoir solutions. Initial screening took place using Hampton Research Crystal Screen. The crystallization conditions obtained were further improved and crystals were routinely obtained using 100 m*M* Tris pH 8.5, 150 m*M* sodium citrate and 20–25% PEG 350, PEG 400 or PEG 550 as the reservoir solution. Rhomboid-shaped crystals with sharp edges of dimensions ∼200 × ∼200 µm were obtained within 7 d (Fig. 1*b*).

4. Data collection and processing

Data were collected by flash-freezing SVV-001 crystals taken directly from the crystallization drop in a liquid-nitrogen cryostream at the BIOCARS beamline 14BMC at APS, Chicago operating under BSL2 conditions. Data were collected on an ADSC Quantum-4 CCD detector using X-rays of wavelength 0.9 Å. A set of 461 high-resolution images were collected in the first pass, with the limit of diffraction reaching beyond 2.3 Å, using an oscillation angle of 0.25° and a crystal-to-detector distance of 400 mm. A low-resolution (100–5 Å) data set of 300 images was obtained in the second pass from the same crystal by moving the detector back to 800 mm and using the same oscillation angle (0.25°). All the images were processed, integrated and scaled in space group *R*3 with unit-cell parameters (in the hexagonal setting) $a = b = 311.5$, $c = 1526.4$ Å, $\alpha = \beta = 90$, $\gamma = 120$° using the *HKL*-2000 suite of programs (Otwinowski & Minor, 1997). The equivalent unit-cell parameters in the primitive rhombohedral

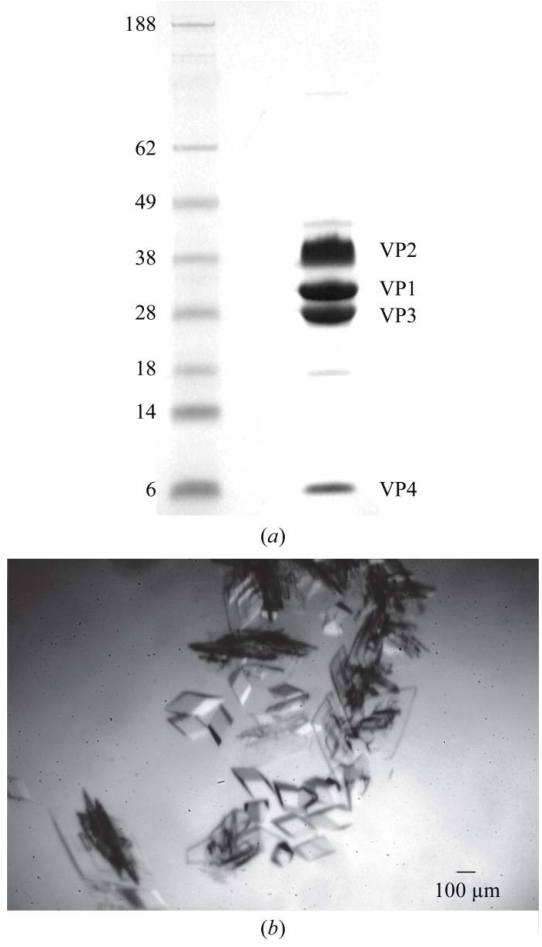

Figure 1
(*a*) SDS–PAGE gel showing the purity of the SVV-001 sample used in crystallization trials. Lane 1 shows the molecular-weight markers (SeeBlue Pre-Stained marker from Invitrogen) and lane 2 shows bands corresponding to VP1, VP2, VP3 and VP4 of the purified SVV-001 sample. (*b*) An image of rhomboid-shaped crystals of SVV-001.

Table 2
Bin statistics.

Resolution	No. of unique observations	$I/\sigma(I)$	Completeness (%)	R_{merge} (%)
92.0–5.0	234541	11.3	95.6	19.4
5.0–4.0	239413	8.7	97.6	17.3
4.0–3.4	238506	7.6	97.2	22.4
3.4–3.1	234009	6.0	95.4	30.2
3.1–2.9	228719	4.4	93.2	44.0
2.9–2.7	212911	3.1	86.8	63.2
2.7–2.6	179386	2.3	73.1	72.6
2.6–2.5	165033	1.7	67.3	82.7
2.5–2.4	144802	1.3	59.0	98.8
2.4–2.3	90966	0.9	37.1	97.1
92.0–2.3	1968286	6.6	80.2	23.3

setting are $a = b = c = 533.0$ Å, $\alpha = \beta = \gamma = 33.6^\circ$. The hexagonal setting was chosen for the ease of performing FFT calculations. The final data set, with a resolution range 92–2.3 Å, contained 1 968 286 unique reflections with an overall completeness and R_{merge} of 80.2% and 23.3%, respectively. *SCALEPACK2MTZ* and *TRUNCATE* (Collaborative Computational Project, Number 4, 1994) were used to convert the integrated intensities into structure-factor amplitudes. The diffraction data displayed $I/\sigma(I) < 2.0$ beyond 2.6 Å resolution. The final data-reduction and bin-wise statistics are shown in Tables 1 and 2, respectively.

5. Preliminary X-ray data analysis

The volume of the SVV-001 *R*3 unit cell in the hexagonal setting suggests that each unit cell accommodates up to six complete virus particles; each particle is composed of 60 protomers. The crystal-packing analysis showed a V_M of 4.52 Å^3 Da^{-1}, corresponding to a solvent content of ∼73% (Matthews, 1968). The volume of the asymmetric unit of the *R*3 space group in the hexagonal setting is one ninth of the volume of the unit cell, as opposed to one third of the volume of the unit cell in the primitive rhombohedral setting. The volume of the rhombohedral cell is one third that of the hexagonal cell. Irrespective of the choice of unit cell, the contents of the asymmetric unit remains the same, consisting of 40 protomers [(6 × 60)/9]. The 40 protomers in the asymmetric unit correspond to two distinct sets of one third of a particle; each set consists of 20 protomers.

The self-rotation function analysis highlighted the presence of fivefold, threefold (Fig. 2*a*) and twofold symmetry, which is the hallmark of icosahedral point-group symmetry (Tong & Rossmann, 1990). The self-rotation function analysis suggested that one of the threefold axes of the particle coincided with the *c* axis of the unit cell, which also represents the crystallographic threefold axis of the *R*3 cell (Fig. 2*a*). Observation of one constellation of (ten) threefold peaks found in the self-rotation function analysis (Fig. 2*a*) using the data between 20 and 5 Å resolution suggested that all the particles in the unit cell are packed in the same orientation.

A one-dimensional locked rotation-function search around the *c* axis was undertaken by pre-aligning one of the particle threefold axes with the *c* axis using the program *GLRF* (Tong & Rossmann, 1990). Interestingly, the locked rotation-function analysis performed using the higher resolution data between 3.2 and 3.0 Å resulted in distinguishing the two orientations of the particles in the unit cell ($\varphi = 0$, $\psi = 0$, $\kappa = 88.4^\circ$) and ($\varphi = 0$, $\psi = 0$, $\kappa = 91.6^\circ$), which were separated by only 3.2° (Fig. 2*b*). This subtle difference in the orientations was only recognized using the higher resolution data. One set of three particles (the first set) in the unit cell are oriented with $\kappa = 88.4^\circ$, while the remaining three particles (the second set) are oriented with $\kappa = 91.6^\circ$; the particles within each individual set are related to each another by the *R*3 symmetry. The accurate positions of the reference particles in each set are under investigation. The peak in between at $\kappa = 90^\circ$ (Fig. 2*b*) appears to be a cross-peak and does not correspond to any particle orientation. This was verified by performing the search with model structure factors using the final solution (results not shown). The locked rotation-function search carried out using the data in the highest resolution bin (2.4–2.3 Å) suggests that there is significant signal (dotted line in Fig. 2*b*) even though $I/\sigma(I)$ is <1 (Table 2). Furthermore, reperforming the self-rotation function analysis (data not shown) using the higher resolution data (3.0–2.4 Å) with finer angular intervals indicated the splitting of each of the threefold peaks

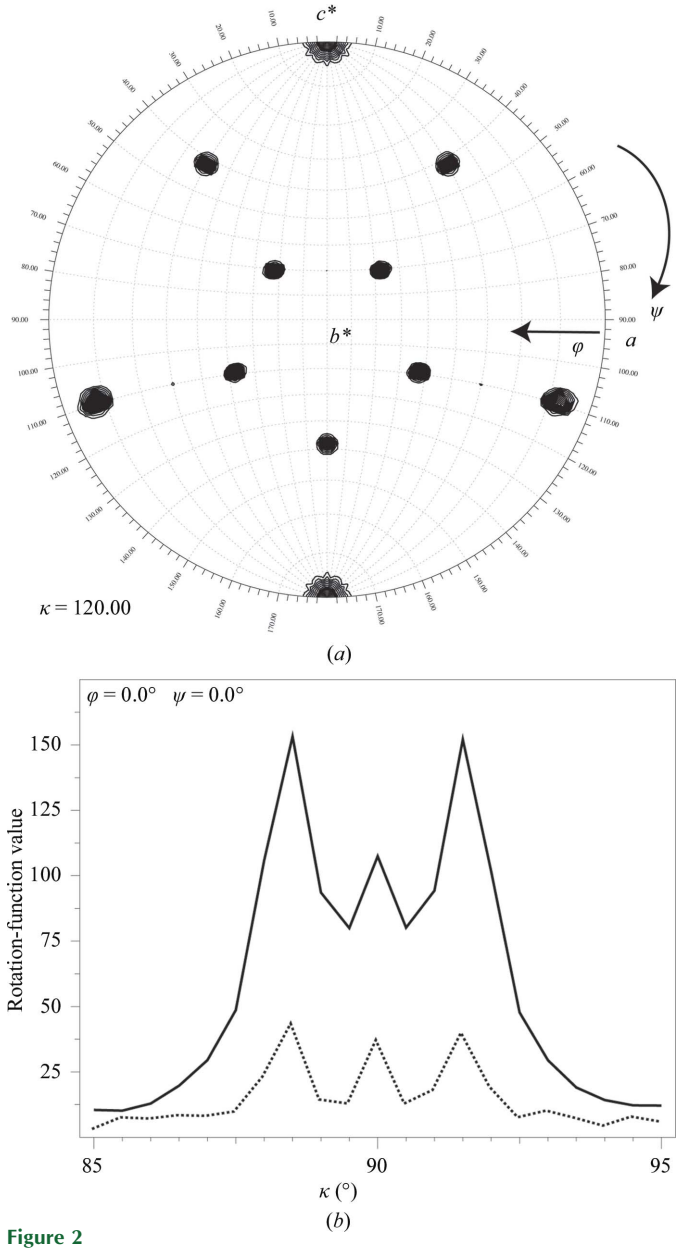

Figure 2
(*a*) A contour plot showing the threefold peaks relative to the unit-cell axis of the SVV-001 crystals. A total of 46 784 large terms in the resolution range 20.0–5.0 Å with a radius of integration of 100 Å were used in the rotation-function calculation. (*b*) The locked rotation-function analysis illustrating the presence of signal in two resolution bins: one between 3.2 and 3.0 Å resolution (solid line) and the highest resolution bin between 2.4 and 2.3 Å (dotted line).

shown in Fig. 2(*a*) into two, confirming that higher resolution data is required to resolve the accurate orientations of the particles in the unit cell.

We are extremely grateful for the assistance and help of the staff at the BIOCARS facility, Drs Vukica Srajer, Reinhard Pahl and Spencer Anderson, in setting up the experiment under the BSL2 conditions. This work was partially supported by NIH grant R56 AI070771 to VSR. Partial salary support to VSR by NIH Research Resource Multi Scale Modeling Tools for Structural Biology (MMTSB), RR12255, is acknowledged.

References

Collaborative Computational Project, Number 4 (1994). *Acta Cryst.* D**50**, 760–763.

Fallaux, F. J., Bout, A., van der Velde, I., van den Wollenberg, D. J., Hehir, K. M., Keegan, J., Auger, C., Cramer, S. J., van Ormondt, H., van der Eb, A. J., Valerio, D. & Hoeben, R. C. (1998). *Hum. Gene Ther.* **9**, 1909–1917.

Hadfield, A. T., Lee, W., Zhao, R., Oliveira, M. A., Minor, I., Rueckert, R. R. & Rossmann, M. G. (1997). *Structure*, **5**, 427–441.

Hales, L. M., Jones, B. H., Vasko, A., Knowles, N. J., Police, S. R. & Hallenbeck, P. L. (2006). *Mol. Ther.* **13**, S187.

Hellen, C. U. T. & de Breyne, S. (2007). *J. Virol.* **81**, 5850–5863.

Knowles, N. J. (2007). Personal communication.

Matthews, B. W. (1968). *J. Mol. Biol.* **33**, 491–497.

Otwinowski, Z. & Minor, W. (1997). *Methods Enzymol.* **276**, 307–326.

Reddy, P. S., Burroughs, K. D., Hales, L. M., Ganesh, S., Jones, B. H., Idamakanti, N., Hay, C., Li, S. S., Skele, K. L., Vasko, A., Yang, J., Watkins, D. N., Rudin, C. M. & Hallenbeck, P. L. (2007). *J. Natl Cancer Inst.* **99**, 1623–1633.

Rossmann, M. G. (1989). *J. Biol. Chem.* **264**, 14587–14590.

Rossmann, M. G., He, Y. & Kuhn, R. J. (2002). *Trends Microbiol.* **10**, 324–331.

Semler, B. L. & Wimmer, E. (2002). Editors. *Molecular Biology of Picornaviruses.* Washington: ASM Press.

Stanway, G., Brown, F., Christian, P., Hovi, T., Hyypiä, T., King, A. M. Q., Knowles, N. J., Lemon, S. M., Minor, P. D., Pallansch, M. A., Palmenberg, A. C. & Skern, T. (2005). *Virus Taxonomy. Eighth Report of the International Committee on Taxonomy of Viruses*, edited by C. M. Fauquet, M. A. Mayo, J. Maniloff, U. Desselberger & L. A. Ball, pp. 757–778. London: Elsevier/Academic Press.

Tong, L. & Rossmann, M. G. (1990). *Acta Cryst.* A**46**, 783–792.